definition

Prosjekt

Group 3: (10025) (10027) (10031) (10032)[a]

[a]*Institutt for matematiske fag, Norges Teknisk-Naturvitenskapelige Universitet, N-7491 Trondheim, Norway.*

Abstract

The Helmholtz equation is in this report discretized with central differences into a five point formula in both cartesian and polar coordinates. Modelled on a finite and an infite domain, with and without an object in the domain. 2nd order convergence was obtained on the unit square in cartesian coordinates. Numerical expriments confimed this and suggested the same order of convergance on an annulus in polar coordinates.

Introduction

Helmholtz Equation

$$\nabla^2 u + \nu^2 u = 0, \ , \tag{1}$$

is a time independent wave equation. Or more specific, it is the fourier transformation of the wave equation to the frequency domain. Even though time is not a variable, the equation can be used to study properties of waves. Therefore, plane waves and scattering around objects will be considered in this report.

First, a finite domain with simple dirichlet boundary conditions will be considered. Discretization of the equation and convergence analysis can then pretty easily be done.

Afterwards, it would be interesting to try to model a more complicated, but more realistic, situation. By, for example, letting a plane wave hit an object $D \subset \mathbb{R}^2$, one can use use the Helmholtz equation to model how the wave will scatter around the object and spread outwards in the plane. To do this, a special set of boundary conditions are needed, called absorbing. Because of the complexity and structure of these boundary conditions, it is convenient to consider a circular grid in polar coordinates. Discretization and a short analysis will therefore follow in polar coordinates, before attacking the scattering case.

1. Discretization of the problem

In two dimentional cartesian coordinates Helmholtz equation is

$$\frac{\partial^2}{\partial^2 x}u + \frac{\partial^2}{\partial^2 y}u + \nu^2 u = 0. \tag{2}$$

For notational purposes, the exact solution will be denoted by u and the approximated solution by U. Applying a grid of M nodes in x-direction and N nodes in y-direction the central difference approximation of the second derivatives are

$$\frac{\partial^2}{\partial^2 x}u_{ij} \approx \frac{1}{\Delta x^2}\left(U_{i+1,j} - 2U_{ij} + U_{i-1,j}\right) \tag{3}$$

at node (i,j) in the grid, where Δx is the step lengths in x direction, and accordingly in the y direction. Inserting these approximations in (2) yields the 5-point-formula

$$\begin{aligned}&\frac{1}{\Delta x^2}\left(U_{i+1,j} + U_{i-1,j}\right) + \frac{1}{\Delta y^2}\left(U_{i,j+1} + U_{i,j-1}\right)\\ &- \left(\frac{2}{\Delta x^2} + \frac{2}{\Delta y^2} - \nu^2\right) U_{i,j} = 0\ .\end{aligned} \tag{4}$$

This gives one equation for each internal node. Including boundary conditions concerning some derivative of u, the total discretization scheme can be written as $A\mathbf{U} = \mathbf{F}$, where $\mathbf{U}$ is a vector of the $U_{i,j}$ points

$$\underset{MN\times 1}{\mathbf{U}} = \begin{bmatrix} U_{1,1} \\ U_{2,1} \\ \vdots \\ U_{M,N} \end{bmatrix}\ , \tag{5}$$

Letting the first M elements of $\mathbf{U}$ correspond to $y = 1$ and so on, the matrix A will be

$$\underset{MN\times MN}{\mathrm{A}} = \begin{bmatrix} B_4 & B_5 & & & & \\ B_3 & B_1 & B_2 & & 0 & \\ & B_3 & B_1 & \ddots & & \\ & & \ddots & \ddots & B_2 & \\ & 0 & & B_3 & B_1 & B_2 \\ & & & & B_6 & B_7 \end{bmatrix}\ , \tag{6}$$

where the B_ks are blocks of size $M \times M$. The diagonals on B_2 and B_3 correspond to the coefficients of the five point formula on the nodes one above and below in y-direction, and B_1 is tridiagonal corresponding to the other three points from equation (4). Row number $M*(j-1)+i$ of A, $\mathbf{U}$ and $\mathbf{F}$ correspond to the equation for point (i,j) on the grid, so when $\mathbf{U}$ is a boundary point the values of the entries in $\mathbf{F}$ and A might differ. This implies that the last element on the subdiagonal and the first element on the superdiagonal of B_1 depend on the specific boundary conditions. The same goes for the first M and last M entries of $\mathbf{F}$ and blocks B_4 through B_7. The rest of entries in $\mathbf{F}$ are zero.

2. Local Truncation error and Stability

The order of the problem can be found by computing the local truncation error (LTE). Exchange the approximations by the exact solutions in the same points, that is $U_{i,j} \to u(x,y)$, $U_{i+1,j} \to u(x+\Delta x, y)$, $U_{i,j+1} \to u(x, y+k)$ and so on. Then use Taylor expansion around (x,y). This yields

$$\begin{aligned} u(x \pm \Delta x, y) = u(x,y) \pm h u_x(x,y) + \\ \frac{\Delta x^2}{2} u_{xx}(x,y) \pm \frac{\Delta x^3}{6} u_{xxx}(x,y) + \\ \frac{\Delta x^4}{24} u_{xxxx}(x,y) \pm \frac{\Delta x^5}{120} + O(\Delta x^6) \end{aligned} \tag{7}$$

in the x-direction and likewise in y-direction. When adding $u(x+\Delta x, y)$ and $u(x-\Delta x, y)$, quite a few terms will cancel. Then dividing on the step size squared and inserting in the 5-point-formula (4) and combining this with (2), the result is that the LTE is

$$\tau_{i,j} = \frac{\Delta x^2}{12} u_{xxxx}(x,y) + \frac{\Delta y^2}{12} u_{yyyy}(x,y) + O(\Delta x^4 + \Delta y^4). \tag{8}$$

Assuming the exact solution u is smooth enough such that the forth derivatives are bounded, one concludes that the method is of second order in both directions, since $\tau_{i,j} = O(\Delta x^2 + \Delta y^2)$.

Then one can also conclude that the method is consistent, since the local truncation error goes to zero as Δx and Δy goes to zero.

Since Lax' stability theorem states that a consistent method is convergent if and only if it is stable, one also has to prove stability in order to obtain convergence for the method.

For an elliptic equation such as the Helmholtz equation, A must be invertible and the inverse must be bounded by a constant C, in some norm, for all step sizes in order for the scheme to be convergent.

If A is invertible, then none of the eigenvalues are equal to zero. To find the eigenvalues, consider first the unit length $[0,1]$ for the one dimensional Laplace equation with $\Delta x = h$, also with Dirichlet boundary conditions, for simplicity purposes. That is

$$u_{xx} = 0 \quad 0 < x < 1 \quad u(0) = \alpha \; u(1) = \beta \tag{9}$$

The Laplace equation is here initially used since the matrix A for this equation,A_L, is similar to A for the Helmholtz equation in the same number of dimensions.

$$A_L = \frac{1}{h^2} \begin{bmatrix} -2 & 1 & & 0 \\ 1 & \ddots & \ddots & \\ & \ddots & \ddots & 1 \\ 0 & & 1 & -2 \end{bmatrix} \tag{10}$$

with known eigenvalues

$$\lambda_j = \frac{2}{h^2} \left[cos\left(j\pi h\right) - 1 \right] \quad j = 1, ..., M \tag{11}$$

which are only zero if the cosine term is one. This only happens if $j \cdot h = 0$ or even multiples of π. Since $h = \frac{1}{M+1}$ and $j = 1, ..., M$, the possible values of $j \cdot h$ lie in the open interval $(0,1)$. Thus the eigenvalues are never exactly zero, and the matrix A_L is invertible.

Now, the matrix must be bounded. Consider for instance the 2-norm: By definition of the norm and using the fact that A_L is symmetric, one obtains $\|A_L\|_2 = \rho(A_L)$ where $\rho(A_L)$ is the spectral radius of A_L. When $\sigma(A_L)$ is the collection of eigenvalues of the matrix, the spectrum, the 2-norm is in this case $\|A_L\|_2 = \max_{\lambda \in \sigma(A_L)} |\lambda|$.

Analogously

$$\|A_L^{-1}\|_2 = \rho(A_L^{-1}) = \max_{\lambda \in \sigma(A_L)} |\lambda^{-1}| = \frac{1}{\min_{\lambda \in \sigma(A_L)} |\lambda|} \tag{12}$$

The cosine term is approximated by the series expansion

$$cos(x) = 1 - \frac{x^2}{2!} + \frac{x^4}{4!} + \mathcal{O}(h^6), \text{with } x = m\pi h. \tag{13}$$

Inserted into the expression for the j-th eigenvalue in (11) one obtains

$$\lambda_j = \frac{2}{h^2} \left(-\frac{(j\pi h)^2}{2!} + \frac{(j\pi h)^4}{4!} + \mathcal{O}(h^6) \right) = -j^2\pi^2 + \mathcal{O}(h^2) \tag{14}$$

and

$$\min_{\lambda \in \sigma(A_L)} |\lambda| = |\lambda_1| = \pi^2 + \mathcal{O}(h^2) \tag{15}$$

such that

$$\|A_L^{-1}\|_2 = \frac{1}{|\lambda_1|} \to \frac{1}{\pi^2}, \quad \text{when } h \to 0. \tag{16}$$

This means that there exists $C > 0$ and $H > 0$ such that $\|A_L^{-1}\|_2 = \frac{1}{|\lambda_1|} < C$ for all $h < H$. Choose for instance $C = \frac{1}{\pi^2} + 1$ and stability is thus proven for one dimensional Laplace equation with the proposed scheme in the 2-norm. Due to equivalence of norms, one has stability for the one dimensional Laplace equation in any norm.

A similar approach is applied when considering the 5-point formula for the Helmholtz equation in two space dimensions. Consider the case $\Delta x = \Delta y = h$.

$$\underset{M^2 \times M^2}{\mathrm{A}} = \frac{1}{h^2} \begin{bmatrix} B & I & & 0 \\ I & \ddots & \ddots & \\ & \ddots & \ddots & I \\ 0 & & I & B \end{bmatrix} \tag{17}$$

with

$$\underset{M\times M}{\mathrm{B}} = \begin{bmatrix} \nu^2-4 & 1 & & 0 \\ 1 & \ddots & \ddots & \\ & \ddots & \ddots & 1 \\ 0 & & 1 & \nu^2-4 \end{bmatrix} \tag{18}$$

and I being the $M \times M$ identity matrix. B can be written as

$$B = (\nu^2 - 2)I + S \tag{19}$$

where $S = A_L$ from equation (10) and has the eigenvalues given in (14). Thus the i-th eigenvalue of B is

$$\lambda_i(B) = \nu^2 - 2 + \lambda_i(S) \tag{20}$$

Denote $\bar{A} = h^2 A$.

Then the eigenvalues of $\bar{A}$ are γ from the equation

$$\bar{A}v = \gamma v \tag{21}$$

It can be shown that (21) can be written as

$$B_\Lambda \omega = \gamma \omega \tag{22}$$

with the same eigenvalues γ in (22) as in (21). This is because B is symmetric and then orthogonal diagonalizable, and as a consequence can be written as $B = V\Lambda V^T$ where $\Lambda = \mathrm{diag}\{\lambda_1, ..., \lambda_M\}$. Then

$$\underset{M^2\times M^2}{\mathrm{B}_\Lambda} = \begin{bmatrix} B_{\lambda_1} & & 0 \\ & \ddots & \\ 0 & & B_{\lambda_M} \end{bmatrix} \tag{23}$$

where the eigenvalues of B_Λ are the eigenvalues of the blocks B_{λ_i}, $i = 1, ..., M$. These blocks have the form $B_{\lambda_i} = (\lambda_i(B) + 2)I + S$, whose eigenvalues then are $(\lambda_i(B) + 2) + \lambda_j(S))$. Get M eigenvalues for each i in B_{λ_i} using (20), letting j run from 1 to M, to obtain the M^2 eigenvalues of B_Λ and thus the eigenvalues of $\bar{A}$:

$$\begin{aligned} \gamma_{ij} &= (\lambda_i(B) + 2) + \lambda_j(S) \\ &= \nu^2 + \lambda_i(S) + \lambda_j(S) \\ &\text{for } i = 1, ...M,\ j = 1, ...M. \end{aligned} \tag{24}$$

Since

$$\bar{A}v = \gamma_{ij}v \implies h^2 Av = \gamma_{ij}v \implies Av = \frac{\gamma_{ij}}{h^2}v \tag{25}$$

the eigenvalues of the matrix A are

$$\begin{aligned} \lambda(A) &= \frac{1}{h^2}\left(\nu^2 + \lambda_i(S) + \lambda_j(S)\right) \\ &\text{for } i = 1, ..., M,\ j = 1, ..., M. \end{aligned} \tag{26}$$

From this it is seen that there in fact is a possibility that an eigenvalue may be zero. However, when using the Taylor expansion from (13), one obtains

$$\begin{aligned} \|A^{-1}\|_2 &= \frac{1}{\min_{i,j\in 1,...,M}(\rho(A))} \\ &= \frac{1}{\min_{i,j}(\nu^2 + \lambda_i(S) + \lambda_j(S))} \\ &= \frac{1}{\min_{i,j}(\nu^2 - \pi^2(i^2 + j^2) + \mathcal{O}(h^2))} \end{aligned} \tag{27}$$

which causes problems for boundedness when $h \to 0$ if the denominator goes to zero. This happens when $\nu = \sqrt{i^2 + j^2}$. Thus, as long as

$$\nu \neq \sqrt{i^2 + j^2} \tag{28}$$

the inverse of A is bounded, and convergence is proven for the proposed 5-point scheme for the Helmholtz equation.

3. Numerical verification

As a first approach to solving the Helmholtz equation, consider the square $[0, 1] \times [0, 1] \subset \mathbb{R}^2$. For later purposes, a regular plane wave will be modeled using the Helmholtz equation. That is, the analytical solution is

$$u(x, y) = P_0 e^{i(ax+by)} \tag{29}$$

Then the total wave number is

$$\nu = \sqrt{a^2 + b^2} \tag{30}$$

[3]

and the function values on the boundary of the square are easily found, resulting in the Dirichlet boundary conditions

$$\begin{aligned} g_{x=0}(y) &= P_0 e^{iby};\ g_{x=1}(y) = P_0 e^{i(a+by)}; \\ g_{y=0}(x) &= P_0 e^{iax};\ g_{y=1}(x) = P_0 e^{i(ax+b)}; \end{aligned} \tag{31}$$

For the implementation, the linear system $A\mathbf{U} = F$ is solved. $\mathbf{U}$ consists only of the unknown inner points of the grid. Therefore a vector containing the values needed for the boundary is added. Call this $\mathbf{G}$. Then the system to be solved can be written on the form $A\mathbf{U} + \mathbf{G} = 0$.

A solution of the problem, with step sizes $\Delta x = \Delta y = 0.005$, and with $a = 2\pi$, $b = 3\pi$ and $P_0 = 1$, is shown in figure 1. Only the imaginary part of the solution is used, so the wave has form of a sine function.

The code for this and other interesting properties are included in the zip file that was handed in with the report. Please open 'readme.txt' for an explanation of what each file contains, or simply run one of the files named 'run_*'.

Having the analytical solution, one can easily find the error of the approximation. Then one can numerically verify that the order is indeed of order 2 in both space directions. This is shown in figure 2. It is the imaginary part of the error that is used.

4. Polar coordinates

4.1. Discretization

In polar cooridinates, Helmholtz equation is written

$$\frac{\partial^2 u}{\partial r^2} + \frac{1}{r}\frac{\partial u}{\partial r} + \frac{1}{r^2}\frac{\partial^2 u}{\partial \theta^2} + \nu^2 u = 0. \tag{32}$$

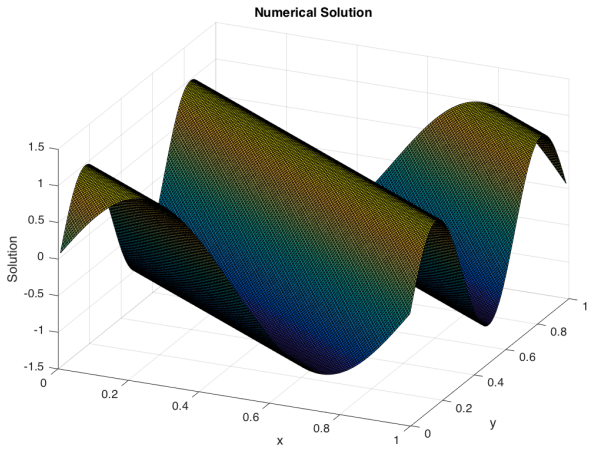

Figure 1: Numerical solution of a plane wave with wave number $\sqrt{(2\pi)^2 + (3\pi)^2}$ on the square $[0,1]x[0,1] \subset \mathbb{R}^2$. The initial amplitude is 1. The grid consists of 200 points in each direction.

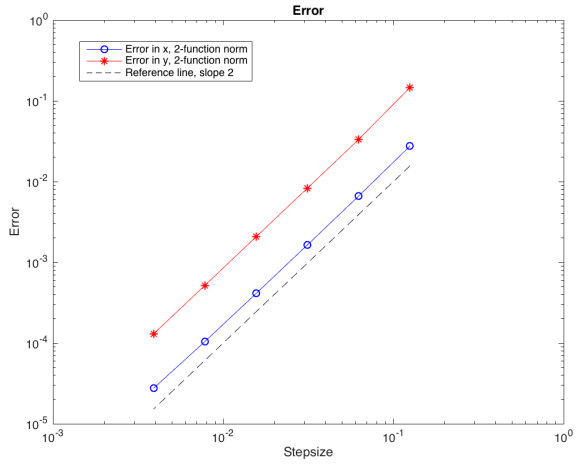

Figure 2: Plot of the error in the numerical solution of a plane wave modelled by Helmholtz equation on the unit square. It shows that the used method is of order two.

Now a circular region is considered, and the grid like that in figure 3 is applied to the region. The grid points are at the places the circular grid curves meet the angular grid lines. Then by using central differences to approximate $\frac{\partial u}{\partial r}$, $\frac{\partial^2 u}{\partial r^2}$ and $\frac{\partial^2 u}{\partial \theta^2}$, the discretization scheme becomes

Here, U_c is the node discretizised around, and r is the corresponding radius. U_t and U_b are nodes with radius $r + \Delta r$ and $r - \Delta r$, respectively. U_r and U_l are the neighboring points in angular direction. Again letting B_4, B_5, B_6, B_7 represent some problem specific boundary conditions the

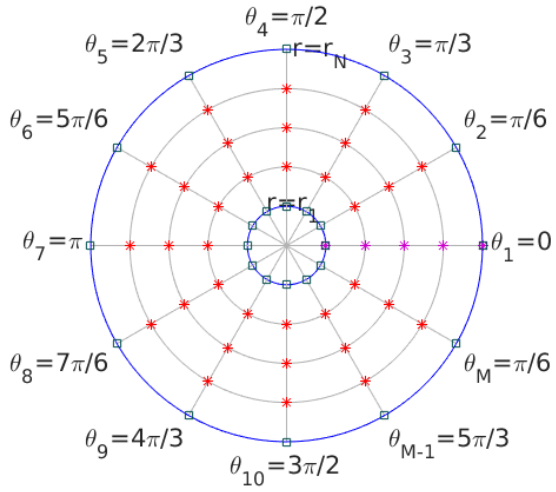

Figure 3: Example of circular grid with M=12 different angles and N=5 radius.

equations can be written in the form $A\mathbf{U} = \mathbf{F}$ with A from equation (6), and the M first elements of $\mathbf{U}$ being the innermost circle on the grid in figure 3, and so on. Notice that B_1 and B_2 will depend on the radius r, such that in the jth blocks of A from the top, the jth radius from the center is used. In the polar case B_1 will not be tridiagonal because the first element of the last column and the last element of the first column will equal $\frac{1}{\Delta\theta^2 r^2}$ to accommodate that gridpoints with the same radius and the 1st and the Mth θ values to be neighbors. Also $\mathbf{F}$ must now be zero except perhaps in the first and last M elements. B_2 and B_3 will again be diagonal matrices and represent respectively the coefficient on the nodes that have a radius that is one step bigger or smaller.

4.2. Convergence

The computation of the local truncation error is very similar to the computation in cartesian coordinates, and ends up concluding that the method is of order two in both directions as long as the third and fourth derivatives in r and forth derivative in θ are bounded and as long as $r \not\to 0$. The stability analysis would be a lot more complex in the polar coordinate case, since the A matrix is not on the exact same form as before. However, we would like to know whether it is likely that we can expect a similar behaviour for the polar coordinates as for the unit square. Therefore, Helmholtz Equation is solved for a plane wave on an annulus, with dirichlet boundary conditions on both outer and inner circle. The inner circle is added to avoid the singularity when $r \to 0$.

The error is more sensitive to stepsize in polar coordinates than in cartesian because of the chosen grid. When the radius increases, the distance between the nodes also increases. Then a smaller step size is needed. Also, the error in θ-direction is in general bigger than in r-direction, also because of the grid. Because of this, the plane wave is modeled on a domain where r is not too big. The inner circle has radius $r_{min} = 1$ and the outer circle har radius

$r_{max} = 5$. Then the domain is still quite large compared to the radius of the inner circle. The resulting error in both directions is shown 5. It is clear that the method does not produce reasonable results for the largest step sizes.

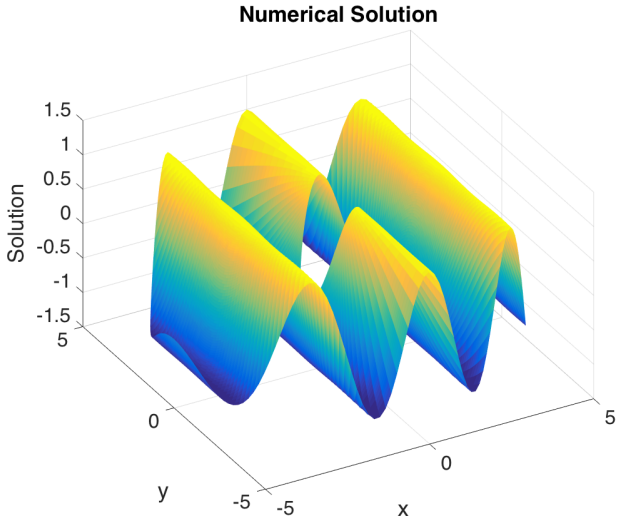

Figure 4: Numerical solution of a plane wave on an annulus.The inner circle has radius $r_{min} = 1$, and outer has radius $r_{max} = 5$. 200 grid points are used in each direction.

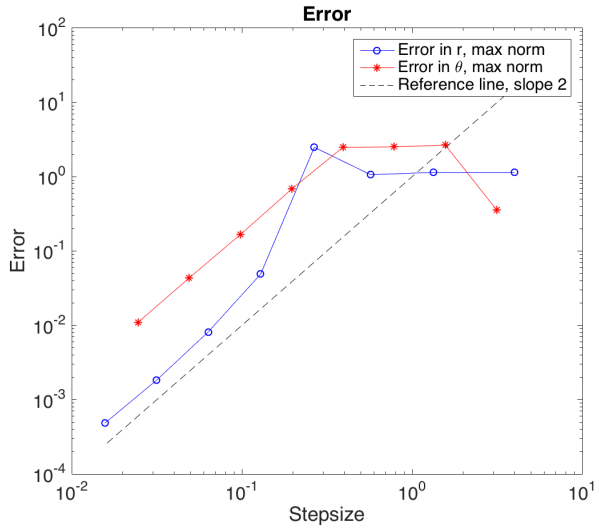

Figure 5: Plot of the error in the numerical solution of a plane wave modelled by Helmholtz equation in polar coordinates. It shows that the used method is of order two for sufficiently small step sizes.

5. Scattering of waves and infinite domain

For modeling scattering of waves around an object, one will use that the total wave, u_{tot} equals the incoming plane wave u_{inc} plus the scattered wave u_s:

$$u_{tot} = u_{inc} + u_s. \tag{33}$$

Here the incoming wave is known and is a solution of the Helmholtz equation. Therefore u_s is the unknown that must be solved for. To do this one needs boundary conditions for the boundary of the object, ∂D.The wave is not allowed to pass through the object, so the component of the derivative normal to the surface should be zero. That is, $\frac{\partial u_{tot}}{\partial n} = 0$. n is the outwards unit normal vector. The conditions for u_s are found from this:

$$\begin{aligned} \frac{\partial u_{inc} + u_s}{\partial n} &= 0 \\ \frac{\partial u_s}{\partial n} &= -\frac{\partial u_{inc}}{\partial n} \end{aligned} \tag{34}$$

In addition to the boundary conditions on the object, it is necessary to have conditions for an outer boundary. One would wish to model the function on an infinite domain were the wave will keep going outwards, but this is of course not possible. Instead, one will choose a finite area of $\mathbb{R}^2$ and model the scattering of the wave there, and add boundary conditions to minimize the reflection of the wave and make it seem like the wave continues outwards. Such boundary conditions are called absorbing, and are to be used on the scattered wave. Some such BCs that are commonly used are the so called Majda and Engquist operators, which was published by American Mathematical Society in 1977 [1], and exist of different orders. Higher orders then absorbing the waves better than lower orders. They can also be found in both cartesian and polar coordinates. However, they are easier to work with in polar coordinates, and it is more convenient to proceed in the circular grid.

The two first Majda and Engquist operators in polar coordinates are

$$E_1 u = (\frac{\partial}{\partial r} - i\nu + \frac{1}{2R})u = 0 \tag{35}$$

$$E_2 u = [\frac{\partial}{\partial r} - (i\nu - \frac{1}{2R}) - (\frac{i}{2\nu R^2} + \frac{1}{2\nu^2 R^3})\frac{\partial^2}{\partial \theta^2}]u = 0 \tag{36}$$

[2] E_1 is of order 1 and E_2 is of order 2. i is the imaginary unit. Looking at a circular domain, one can implement these conditions on the whole outer boundary. Not having to consider different conditions and not having any corners or points on the boundary where the derivatives do not exist, is a great advantage, and the reason why we have implemented a grid in polar coordinates.

It would be interesting to see how the order of the operators affect the solutions, therefore we would like to model the scattering with both boundary conditions.

Letting the first order Majda and Engquist operator work on the scattered wave that is to be modelled, yields

$$\frac{\partial}{\partial r} u_s + (-i\nu + \frac{1}{2R})u_s = 0\ . \tag{37}$$

Not to lose accuracy in the solution compared to the 5-point-formula already implemented, a second order approximation of the derivative is needed. We get

$$\frac{\partial}{\partial r} u_s \approx \frac{U_s(r + \Delta r, \theta) - U_s(r - \Delta r, \theta)}{2\Delta r}. \tag{38}$$

Since this is on the outer boundary, $U_s(r+\Delta r,\theta)$ is outside the considered domain. Thus this must be eliminated. One can then solve (32) for $U_s(r+\Delta r,\theta)$ and insert in (38) to get

$$\begin{aligned}\frac{\partial u(R,\theta)}{\partial r} &\approx U_R = \\ &-\frac{1}{2\Delta r}\Big(\frac{1}{\Delta r^2}+\frac{1}{2\Delta r R}\Big)^{-1}\Big(\frac{1}{\Delta\theta^2 R^2}U_s(R,\theta-\Delta\theta)\\ &+\frac{1}{h^2R^2}U_s(R,\theta+\Delta\theta)+U_s(R,\theta)\Big(-\frac{2}{\Delta r^2}-\frac{2}{\Delta\theta^2 r^2}+\nu^2\Big)\Big)\\ &-\frac{U_s(R-\Delta r,\theta)}{2\Delta r}\Big(1+\Big(\frac{1}{\Delta r^2}+\frac{1}{2\Delta r R}\Big)^{-1}\Big(\frac{1}{\Delta r^2}-\frac{1}{2\Delta r R}\Big)\Big),\end{aligned} \tag{39}$$

where R is the outer radius of the domain. In total we have

$$U_R+(-i\nu+\frac{1}{2R})U_s(R,\theta)=0\,. \tag{40}$$

For the second order operator, a second order approximation of $\frac{\partial^2}{\partial\theta^2}$ as well as $\frac{\partial}{\partial r}$ is needed. For the outer boundary we get

$$\frac{\partial^2}{\partial\theta^2}u_s(R,\theta)\approx\frac{1}{\Delta\theta^2}(U_s(R,\theta-\Delta\theta)+U_s(R,\theta+\Delta\theta)-2U_s(R,\theta))\,, \tag{41}$$

where $\Delta\theta=\frac{2\pi}{M}$

Then it is easy to combine the expressions in a similar way as with first order conditions.

Then focusing on an incoming wave hitting an object in the domain. Specifically, investigate how a plane wave scatters around a circular object in an infinite plane. Placing the object at the center of a circular grid, the grid can be expressed as in figure 3. The incoming wave that will hit the object is

$$u_{inc}=P_0\,e^{i\,\nu\,r\cos(\theta)}, \tag{42}$$

and we have

$$\frac{\partial u_{inc}}{\partial r}=P_0e^{i\nu rcos(\theta)}i\nu cos(\theta). \tag{43}$$

Since the object is a circle, the normal derivative on the object is just the derivative with respect to r. So from the condition $\frac{\partial}{\partial n}u_{tot}=0$, we get

$$\frac{\partial}{\partial r}u_s=-\frac{\partial}{\partial r}u_{inc}=-P_0e^{i\nu rcos(\theta)}i\nu cos(\theta). \tag{44}$$

Discretization of the derivative on the boundary of the object is done the same way as for the outer boundary: second order discretization with fictitious node. The only difference is that the node to be eliminated is the node below, so the scheme is slightly different.

The solutions are shown in figures 6, 7 and 8, all with amplitude $P_0=1$, radius of inner circle $r_{min}=3$, radius of outer circle $r_{max}=12$ and wave number $nu=\frac{2\pi}{3}$. There are $m=n=600$ steps in both space directions.

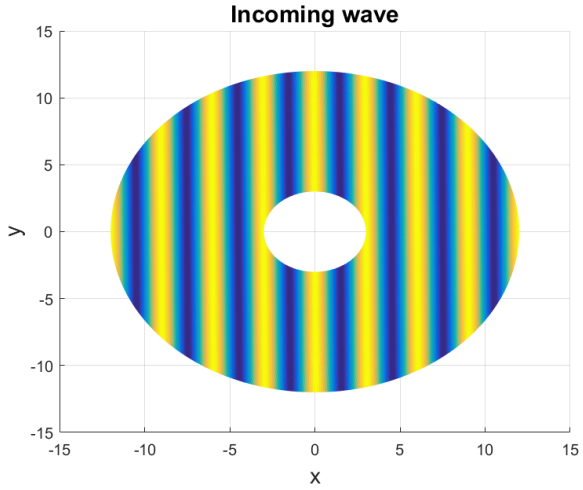

Figure 6: The analytical solution of a plane wave propagating in positive x direction. Amplitude $P_0=1$, wave number $\nu=\frac{2\pi}{3}$, radius of object $r_{min}=3$, and radius of domain $r_{max}=12$.

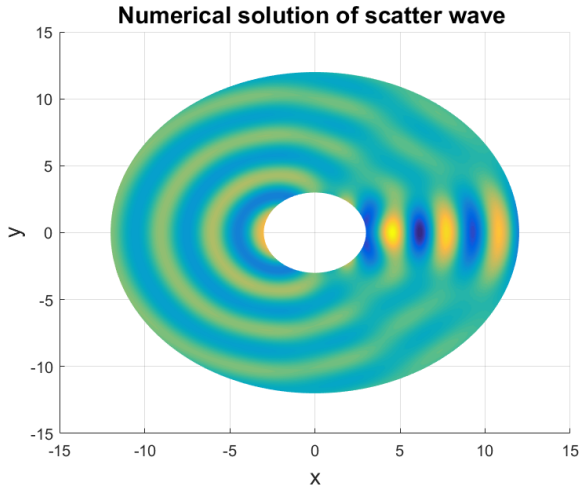

Figure 7: Numerical solution of the scatter wave, when the plane wave has hit the object and spread. Amplitude $P_0=1$, wave number $\nu=\frac{2\pi}{3}$, radius of object $r_{min}=3$, and radius of domain $r_{max}=12$.

These plots show the how the comes into the domain, how it hits the object and spreads and how the resulting wave looks. Error plots to show convergence are shown in the following. The analytical solution [2] of the scatter wave is used as a reference solution.

Here, the values for amplitude, wave number and inner and outer boundary are the same as for the polar coordinate case with Dirichlet boundary conditions. Number of steps are $n=2^q$, $q=3,...,9$ and $m=2^{12}$ for both first and second order absorbing boundary operator for the error in r. For the error in *theta*: $m=2^q$, $q=3,...,9$ and $n=2^{12}$.

As one might from the order of discretization and from the results from the finite domain with Dirichlet boundary

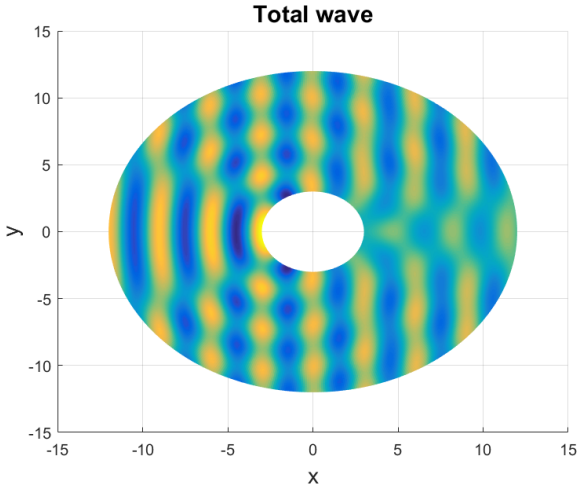

Figure 8: Total wave, the sum of the incoming plane wave and the scatter wave after hitting the object. Amplitude $P_0 = 1$, wave number $\nu = \frac{2\pi}{3}$, radius of object $r_{min} = 3$, and radius of domain $r_{max} = 12$.

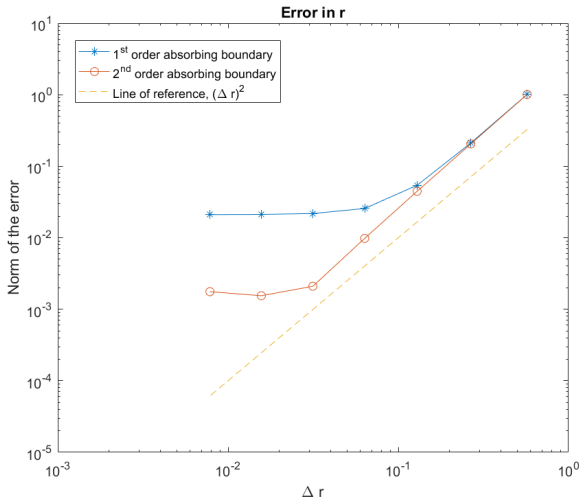

Figure 9: Error plot for r where Δr is plotted against the frobenius norm of the absolute difference between the analytical and numerical solution. Number of steps are $n = 2^q,\ q = 3, ..., 9$ and $m = 2^{12}$.

conditions, second order convergence is obtained overall. However, for small step lengths, the error in the absorbing boundary operators starts to interfere with the precision of the numerical solution. This gives a bended curve in the lower left part of the graphs since the error then does not decrease at the same rate. The operator of order one starts to affect the solution for bigger step sizes than the operator of second order, and therefore stabilizes at a bigger error in the plot, over the curve for the error for the operator of second order. The same trend is seen in both the convergence plot for r and the plot for θ.

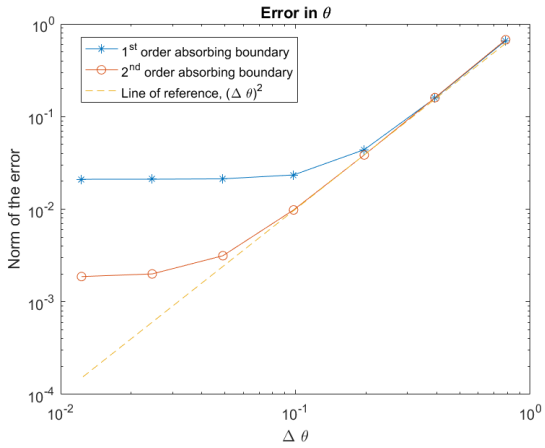

Figure 10: Error plot for θ where $\Delta\theta$ is plotted against the frobenius norm of the absolute difference between the analytical and numerical solution. Number of steps are $m = 2^q,\ q = 3, ..., 9$ and $n = 2^{12}$

6. Conclusion

Helmholtz equation was discretized with central differences to a five point formula in both cartesian and polar coordinates. The theoretical properties were investigated for a simple finite domain in cartesian coordinates and resulted in an expected second order of convergence. This result was supported in numerical experiments. Numerical experiments on a finite domain in polar coordinates also resulted in second order convergence, which indicated a similar behavior for polar coordinates although this was not shown theoretically. This was also as expected since all approximations were done in second order. When modelling an infinite domain, absorbing Majda and Engquist boundary operators were used on the outer boundary. Both the first and second order Majda Engquist operators were used. Second order convergence was again obtained. Now, the accuracy of the absorbing boundary conditions was clearly visible in the error plots, where the accuracy of the absorption became dominating when the step size decreased. The increased prescision from utilizing the second order operator is considerable.

The project work has been somewhat difficult due to illness. 10025, 10027, 10032 have contributed equally to the project. 10031 has not been able to do so due to the aforementioned illness. She has however put considerable effort into the project, particularly a part about waves scattered on a triangle in a cartesian grid. The work on this part is not yet finished, and so it is not included in the report.

Referanser

[1] B. Engquist and A. Majda, Absorbing boundary conditions for the numerical simulation of waves, Math. Comp. 31, No. 139, 629–651 (1977).
[2] F. Ihlenburg. Finite element analysis of acoustic scattering, p. 30 and p. 76. Springer-Verlag, New York (1998)

[3] D. Givoli. Numerical methods for problems in infinite domains, p. 56, Elsevier (1992)